

Dipole Illumination Model Correction

Talon Chandler

March 24, 2017

1 Summary

Our current model for the induced dipole moment created by illuminating a single fluorophore with a monochromatic plane wave is

$$\boldsymbol{\mu}_{\text{ind}} \propto \hat{\boldsymbol{\mu}}_{\text{em}} [\hat{\boldsymbol{\mu}}_{\text{abs}} \cdot \mathbf{E}]. \quad (1)$$

In these notes I will re-derive this model and correct several errors. The corrected model is

$$\boldsymbol{\mu}_{\text{ind}} \propto \hat{\boldsymbol{\mu}}_{\text{em}} \left| \hat{\boldsymbol{\mu}}_{\text{abs}}^\dagger \mathbf{A} \right| \quad (2)$$

where \mathbf{A} is the complex envelope (also known as the generalized Jones vector).

2 Math Preliminaries

2.1 Set Definitions

\mathbb{R} : the set of real numbers

\mathbb{R}^n : the set of n dimensional vectors with real components

\mathbb{C} : the set of complex numbers

\mathbb{C}^n : the set of n dimensional vectors with complex components

$\mathbb{S}^n = \{x \in \mathbb{R}^n : |x| = 1\}$: the set of real unit vectors in n dimensions.

$\mathbb{T}^n = \{x \in \mathbb{C}^n : |x| = 1\}$: the set of complex unit vectors in n dimensions.

$[a, b) = \{x \in \mathbb{R} : a \leq x < b\}$: shorthand for subsets of the real numbers.

2.2 Useful Operations With Complex Vectors

Consider $\mathbf{x}, \mathbf{y} \in \mathbb{C}^n$.

1. The conjugate transpose of \mathbf{x} is denoted by a dagger (\mathbf{x}^\dagger).
2. $|\mathbf{x}|^2 = \mathbf{x}^\dagger \mathbf{x}$.
3. $\mathbf{x}^\dagger \mathbf{y} = \mathbf{x} \cdot \mathbf{y}$ if $\mathbf{x}, \mathbf{y} \in \mathbb{R}^n$
4. $(\mathbf{x} \mathbf{y}^\dagger)^\dagger = \mathbf{y} \mathbf{x}^\dagger$

3 Representations of Polarized Plane Waves

The time dependent electric field \mathcal{E} of a polarized monochromatic plane wave is given by

$$\mathcal{E}(\mathbf{r}, t) = E_{o,x} \cos(k_x r_x - \omega t) \hat{\mathbf{x}} + E_{o,y} \cos(k_y r_y - \omega t - \varphi_y) \hat{\mathbf{y}} + E_{o,z} \cos(k_z r_z - \omega t - \varphi_z) \hat{\mathbf{z}} \quad (3)$$

where $\mathbf{E}_o = [E_{o,x}, E_{o,y}, E_{o,z}]^T \in \mathbb{R}^3$ is the real electric field amplitude, $\mathbf{k} = [k_x, k_y, k_z]^T \in \mathbb{R}^3$ is the wave vector which points in the direction of propagation, $\mathbf{r} = [r_x, r_y, r_z]^T \in \mathbb{R}^3$ is the position, $\omega \in \mathbb{R}$ is the angular frequency, and φ_y (φ_z) $\in [0, 2\pi)$ is the phase shift of the y (z) component. For equation 3 to represent a

physically realizable polarized plane wave, we require that $\mathbf{E} \cdot \mathbf{k} = 0$ so that the plane wave is transverse, and $|\mathbf{k}| = \frac{\omega}{c}$ so that the wave can propagate.

The complex spatial electric field \mathbf{E} for a monochromatic polarized plane wave is given by

$$\mathbf{E}(\mathbf{r}) = \mathbf{A}e^{j\mathbf{k} \cdot \mathbf{r}} \quad (4)$$

where $\mathbf{E} \in \mathbb{C}^3$, and $\mathbf{A} \in \mathbb{C}^3$ is the complex envelope. We can recover the time dependent electric field from the complex spatial electric field using

$$\mathcal{E}(\mathbf{r}, t) = \text{Re} \{ \mathbf{E}(\mathbf{r})e^{-j\omega t} \} \quad (5)$$

We can view equation 4 as a factorization of \mathbf{E} into a spatially dependent part ($e^{j\mathbf{k} \cdot \mathbf{r}}$) and a spatially independent part (\mathbf{A}). \mathbf{A} is called the complex envelope [1] or the generalized Jones vector [2]. The conventional Jones vector \mathbf{J} only considers polarized plane waves traveling along the z axis, so $\mathbf{J} \in \mathbb{C}^2$ suffices to describe the polarization state. \mathbf{A} describes the polarization state for plane waves traveling in any direction, so $\mathbf{A} \in \mathbb{C}^3$ is required.

4 Power Absorbed By A Dipole

The power absorbed by a single dipole with absorption dipole moment $\boldsymbol{\mu}_{\text{abs}}$ illuminated by a polarized plane wave is [3]

$$P_{\text{abs}} \propto |\hat{\boldsymbol{\mu}}_{\text{abs}}^\dagger \mathbf{E}|^2 \quad (6)$$

where $\hat{\boldsymbol{\mu}}_{\text{abs}} \in \mathbb{T}^3$ is the absorption dipole moment. Notice that we've allowed $\hat{\boldsymbol{\mu}}_{\text{abs}}$ to be a unit complex vector instead of restricting it to be a unit real vector. Although we'll focus on the case of $\hat{\boldsymbol{\mu}}_{\text{abs}} \in \mathbb{S}^3$ experimentally, allowing $\hat{\boldsymbol{\mu}}_{\text{abs}} \in \mathbb{T}^3$ simplifies the notation and allows us to consider complex transition moments (transitions that are excited by circularly polarized light) if required.

4.1 Absorbed Power Is Independent of Phase

Equation 6 extends to generalized Jones vectors. Plugging 4 into 6 and using the operations in section 2.2 gives

$$P_{\text{abs}} \propto |\hat{\boldsymbol{\mu}}_{\text{abs}}^\dagger \mathbf{A}e^{j\mathbf{k} \cdot \mathbf{r}}|^2 \quad (7)$$

$$P_{\text{abs}} \propto (\hat{\boldsymbol{\mu}}_{\text{abs}}^\dagger \mathbf{A}e^{j\mathbf{k} \cdot \mathbf{r}})^\dagger (\hat{\boldsymbol{\mu}}_{\text{abs}}^\dagger \mathbf{A}e^{j\mathbf{k} \cdot \mathbf{r}}) \quad (8)$$

$$P_{\text{abs}} \propto (\hat{\boldsymbol{\mu}}_{\text{abs}}^\dagger \mathbf{A})^\dagger (\hat{\boldsymbol{\mu}}_{\text{abs}}^\dagger \mathbf{A})e^{j\mathbf{k} \cdot \mathbf{r}}e^{-j\mathbf{k} \cdot \mathbf{r}} \quad (9)$$

$$P_{\text{abs}} \propto |\hat{\boldsymbol{\mu}}_{\text{abs}}^\dagger \mathbf{A}|^2 \quad (10)$$

This confirms Rudolph and Shalin's claim that absorbed power is independent of phase.

4.2 Sum Over Source

Finally, we show that if a dipole is illuminated by two plane waves with independent phase (say by two lasers that are not phase locked, or by illuminating two points on the back focal plane of a condenser with a thermal source) then the total absorbed power is the sum of the absorbed powers due to the individual plane waves. Let \mathbf{E}_1 and $\mathbf{E}_2 \exp\{j\phi\}$ be the complex spatial electric fields created by the first and second illuminating plane waves where $\phi \sim U(0, 2\pi)$ is a uniformly distributed phase difference between the two plane waves. The expected

value of the absorbed power is

$$E[P_{\text{abs}}] \propto E \left[|\hat{\boldsymbol{\mu}}_{\text{abs}}^{\dagger} (\mathbf{E}_1 + \mathbf{E}_2 \exp\{j\phi\})|^2 \right] \quad (11)$$

$$E[P_{\text{abs}}] \propto E \left[\left[\hat{\boldsymbol{\mu}}_{\text{abs}}^{\dagger} (\mathbf{E}_1 + \mathbf{E}_2 \exp\{j\phi\}) \right]^{\dagger} \left[\hat{\boldsymbol{\mu}}_{\text{abs}}^{\dagger} (\mathbf{E}_1 + \mathbf{E}_2 \exp\{j\phi\}) \right] \right] \quad (12)$$

$$E[P_{\text{abs}}] \propto E \left[\left[\hat{\boldsymbol{\mu}}_{\text{abs}}^{\dagger} (\mathbf{E}_1 + \mathbf{E}_2 \exp\{j\phi\}) (\mathbf{E}_1^{\dagger} + \mathbf{E}_2^{\dagger} \exp\{-j\phi\}) \hat{\boldsymbol{\mu}}_{\text{abs}} \right]^{\dagger} \right] \quad (13)$$

$$E[P_{\text{abs}}] \propto E \left[\left[\hat{\boldsymbol{\mu}}_{\text{abs}}^{\dagger} (\mathbf{E}_1 \mathbf{E}_1^{\dagger} + \mathbf{E}_2 \mathbf{E}_1^{\dagger} \exp\{j\phi\} + \mathbf{E}_1^{\dagger} \mathbf{E}_2 \exp\{-j\phi\} + \mathbf{E}_2 \mathbf{E}_2^{\dagger}) \hat{\boldsymbol{\mu}}_{\text{abs}} \right]^{\dagger} \right] \quad (14)$$

Pulling the expectation inside and using $E[\exp\{j\phi\}] = 0$ gives

$$E[P_{\text{abs}}] \propto \left[\hat{\boldsymbol{\mu}}_{\text{abs}}^{\dagger} (\mathbf{E}_1 \mathbf{E}_1^{\dagger} + \mathbf{E}_2 \mathbf{E}_2^{\dagger}) \hat{\boldsymbol{\mu}}_{\text{abs}} \right]^{\dagger} \quad (15)$$

$$E[P_{\text{abs}}] \propto \left[\hat{\boldsymbol{\mu}}_{\text{abs}}^{\dagger} \mathbf{E}_1 \mathbf{E}_1^{\dagger} \hat{\boldsymbol{\mu}}_{\text{abs}} + \hat{\boldsymbol{\mu}}_{\text{abs}}^{\dagger} \mathbf{E}_2 \mathbf{E}_2^{\dagger} \hat{\boldsymbol{\mu}}_{\text{abs}} \right]^{\dagger} \quad (16)$$

$$E[P_{\text{abs}}] \propto |\hat{\boldsymbol{\mu}}_{\text{abs}}^{\dagger} \mathbf{E}_1|^2 + |\hat{\boldsymbol{\mu}}_{\text{abs}}^{\dagger} \mathbf{E}_2|^2 \quad (17)$$

$$E[P_{\text{abs}}] \propto P_{\text{abs},1} + P_{\text{abs},2} \quad (18)$$

This confirms Rudolph and Shalin's claim that independent plane waves excite a fluorophore independently. We can extend the argument to an arbitrary number of independent plane waves which allows us to integrate over all plane waves incident on the fluorophore to find the total absorbed power.

5 Dipole Emission Pattern

The emitted electric field pattern is proportional to the Green's tensor multiplied by the emission dipole moment of the fluorophore

$$\mathbf{E}_{\text{em}}(\mathbf{r}) \propto \mathbf{G} \hat{\boldsymbol{\mu}}_{\text{em}}. \quad (19)$$

where $\hat{\boldsymbol{\mu}}_{\text{em}} \in \mathbb{T}^3$. The power emitted by a fluorophore is proportional to the power absorbed

$$P_{\text{em}} \propto P_{\text{abs}}. \quad (20)$$

Using equation $P_{\text{em}} \propto |\mathbf{E}_{\text{em}}(\mathbf{r})|^2$ and 10 gives

$$|\mathbf{E}_{\text{em}}(\mathbf{r})|^2 \propto |\hat{\boldsymbol{\mu}}_{\text{abs}}^{\dagger} \mathbf{A}|^2. \quad (21)$$

Taking the square root of 21 and combining with 19 gives the final result

$$\mathbf{E}_{\text{em}}(\mathbf{r}) \propto \mathbf{G} \hat{\boldsymbol{\mu}}_{\text{em}} |\hat{\boldsymbol{\mu}}_{\text{abs}}^{\dagger} \mathbf{A}|. \quad (22)$$

6 Induced Dipole Moment

We can split equation 22 into two parts using the induced dipole moment

$$\boldsymbol{\mu}_{\text{ind}} \equiv \hat{\boldsymbol{\mu}}_{\text{em}} |\hat{\boldsymbol{\mu}}_{\text{abs}}^{\dagger} \mathbf{A}| \quad (23)$$

$$\mathbf{E}_{\text{em}}(\mathbf{r}) \propto \mathbf{G} \boldsymbol{\mu}_{\text{ind}} \quad (24)$$

where $\boldsymbol{\mu}_{\text{ind}} \in \mathbb{C}^3$.

7 Köhler Illumination

The work in these notes extends to the previous note set. The induced dipole moment created by Köhler illumination is given by

$$\boldsymbol{\mu}_{\text{ind}} \propto \boldsymbol{\mu}_{\text{em}} \int d\mathbf{r}' \left| \boldsymbol{\mu}_{\text{abs}}^\dagger \mathbf{R}(\mathbf{r}') \mathbf{A}_{\text{bfp}} \right| \quad (25)$$

Shalin suggested that we separate the model into three parts by moving $\boldsymbol{\mu}_{\text{em}}$ and $\boldsymbol{\mu}_{\text{abs}}$ outside of the integral. This would allow us to calculate the “effective electric field” or “polarization resolved electric field”. The addition of the absolute value bars prevent us from making this simplification.

With equation 25 in view, we can see why the absolute value bars are required. Without the absolute value bars, $\boldsymbol{\mu}_{\text{abs}}^\dagger(\mathbf{r}) \mathbf{R}_s(\mathbf{r}') \mathbf{A}_{\text{bfp}} \in [-1, 1]$, so the integral can evaluate to zero. With the absolute value bars, $|\boldsymbol{\mu}_{\text{abs}}^\dagger(\mathbf{r}) \mathbf{R}_s(\mathbf{r}') \mathbf{A}_{\text{bfp}}| \in [0, 1]$ and each point in the back focal plane contributes to the induced dipole moment.

8 Total Power Emitted By A Dipole

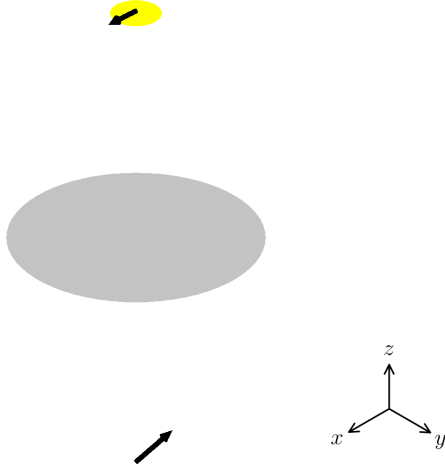


Figure 1: Scene schematic. A single dipole (see arrow in the front focal plane) under x -polarized Köhler illumination (see arrow in the back focal plane).

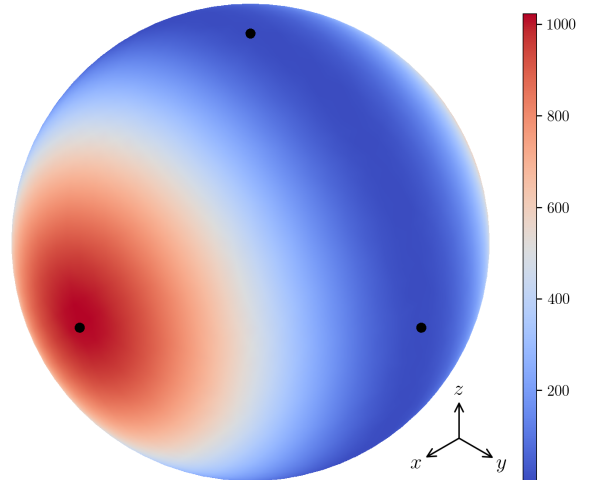


Figure 2: Total power emitted by a single dipole ($|\boldsymbol{\mu}_{\text{ind}}|^2$) as a function of direction under the illumination geometry in Figure 1. Dots indicate where the Cartesian axes intersect the sphere. Arbitrary units.

Figure 1 shows a simple Köhler illumination geometry where x -polarized light illuminates a dipole with the optical axis along z . Figure 2 shows the total power emitted by the dipole as a function of its direction. In practice, we will only collect a fraction of the total power emitted, but Figure 2 shows the total power—as if we had detectors on all sides of the dipole. We can see that dipoles aligned along the x axis will emit (and absorb) the most power, while dipoles aligned along the y or z axes will emit very little power.

Figure 3 shows the total power emitted by a single dipole under different back aperture radii, ρ , with constant illumination power. Our model assumes that the lens is large enough to map each point in the back focal plane

to a plane wave in the front focal plane, so the only parameter of interest is $\frac{\rho}{f}$, the ratio of the back aperture radius to the focal length of the lens.

Figure 3 also shows how the results change when we neglect (second row) and keep (third row) the absolute value bars inside the integral in equation 25. When we neglect the absolute value bars, the model predicts that as we open the back aperture the emitted power pattern is not mirror symmetric about the $x - y$ plane. When we keep the absolute value bars, the absorbed power pattern is symmetric about the $x - y$ plane. Also, notice that $+z$ and $-z$ aligned dipoles emit more power as we open the back aperture (you may have to zoom in on the bottom row to see the difference—the $+z$ axis in the bottom right plot is ~ 300 compared to ~ 0 in the bottom left plot).

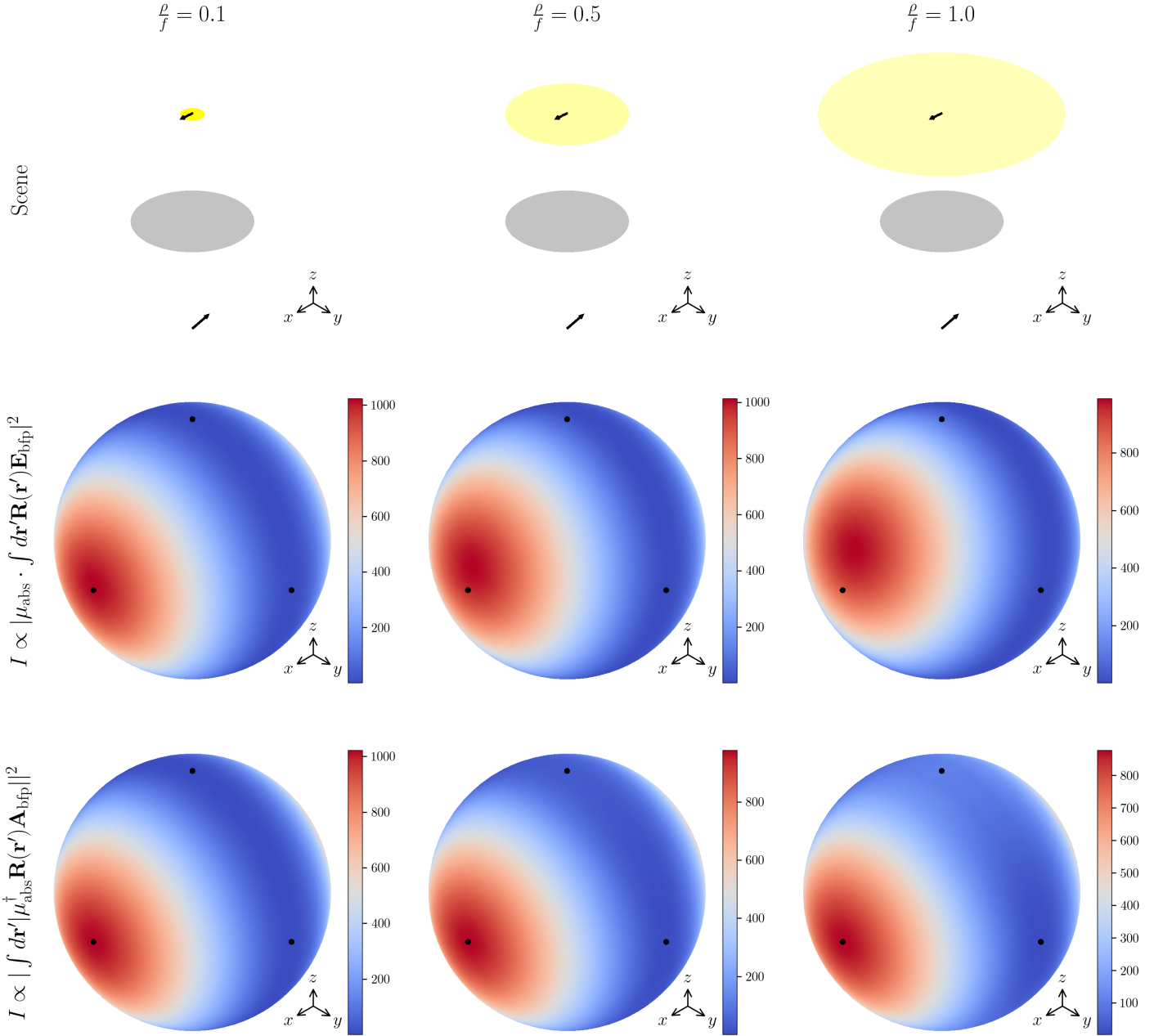


Figure 3: Top row—schematics of the illumination geometries. Middle row—**incorrect** emitted power pattern if the absolute value bars are neglected. Bottom row—**correct** emitted power pattern if the absolute value bars are retained. Columns—the back aperture radius increases from left to right.

9 Aside: Generalized Jones Vectors

The generalized Jones vector in equation 4 is going to be extremely useful for analyzing light fields traveling through crystals. Ortega [4] and Azzam [2] have started developing the generalized Jones calculus, but they haven't applied the results to stacks of crystals. Foreman and Torok [5] have used generalized Jones vectors to analyze high-NA imaging systems, but they haven't applied their results to transmission microscopes like the LC-PolScope. More progress on this front soon!

References

- [1] B.E.A. Saleh and M.C. Teich. *Fundamentals of Photonics*. Wiley Series in Pure and Applied Optics. Wiley, 2007.
- [2] R. M. A. Azzam. Three-dimensional polarization states of monochromatic light fields. *J. Opt. Soc. Am. A*, 28(11):2279–2283, Nov 2011.
- [3] Lukas Novotny and Bert Hecht. *Principles of nano-optics*. Cambridge University Press, 2006.
- [4] Noé Ortega-Quijano and José Luis Arce-Diego. Generalized jones matrices for anisotropic media. *Opt. Express*, 21(6):6895–6900, Mar 2013.
- [5] Matthew R. Foreman and Peter Torok. Computational methods in vectorial imaging. *Journal of Modern Optics*, 58(5-6):339–364, 2011.